Journal of Thermal Analysis, Vol. 52 (1998) 293-313

REVERSIBLE MELTING OF SEMI-CRYSTALLINE POLYMERS
Frequency dependence of the reversible melting enthalpy

F. Cser[*1], *F. Rasoul*[2] *and E. Kosior*[3]

CRC for Polymers Pty. Ltd., 32 Business Park Dr., Notting Hill VIC 3168, Australia

(Received August 19, 1997)

Abstract

Modulated DSC (MDSC) has been used to study the heat flow during melting and crystallisation of some semi-crystalline polymers i.e. different grades of polyethylene (LDPE, LLDPE and HDPE), and polypropylene (PP).

The heat capacities measured by MDSC are compared with the hypothetical complex heat capacities of Schawe and it is shown that numerically they are equivalent; nevertheless, the concept of the complex heat capacity is problematic on a thermodynamic basis.

A reversing heat flow (proportional to the experimental heat capacity of the material) was present at all conditions used for the study. In the melting zone of the polymers it depends on the modulation frequency and on the amplitude. Higher amplitude and frequency of modulation reduce the ratio of the reversing heat flow to the total heat flow, the latter is nearly independent on these parameters.

The reversible component of the melting enthalpy of polymers depends on the modulation frequency, the modulation amplitude and the type of the polymer. It increases by increasing the branching in polyethylene.

The existence of the reversible heat flow during the crystallisation and melting is contrary to the current hypotheses and theories of polymer crystallisation.

Keywords: crystallisation, heat capacity, MDSC, melting, polymers

Introduction

Basics of MDSC

Modulated DSC (MDSC), developed by Reading *et al.* [1, 2] and produced by TA Instruments, combines the linear change of the temperature in a DSC cell

* Author to whom all correspondence should be addressed.
1 Postal address: Dept. Materials Eng. Monash University, Clayton VIC 3168, Australia
2 Recent Address: Chiron Mimotopes, P.O Box 1415, Clayton South VIC 3169, Australia
3 Postal Address: Polymer Technology Center, RMIT, Melbourne VIC 3001, Australia

1418–2874/98/ $ 5.00
© 1998 Akadémiai Kiadó, Budapest
Akadémiai Kiadó, Budapest
Kluwer Academic Publishers, Dordrecht

with a sinusoidal modulation. The equipment records the actual (modulated) temperature, the actual (modulated) heat flow and the phase angle of these two harmonic functions. If the change of the temperature is within the harmonic range (which depends on the parameters of the modulation, the actual temperature and the overall heating rate), then the Fourier analyses of the response to the temperature function results in two functions: the heat capacity (C_p, which is determined mainly by the amplitude of the responses) and the total heat flow (which is the average of the heat flow) [1–4].

Reading *et al.* gave two differential equations as approximations for the total heat flow (Eqs (1a) and (1b)) and after their solution the results can be broken in two parts, i.e. into a reversing (reversible) and a kinetic (or non reversible) heat flows [1, 2]:

$$\Phi(t) = \left(\frac{dQ}{dt}\right)_{total} = C_p(T)\frac{dT}{dt} + f(t,T) \tag{1a}$$

$$\Phi(t) = [C_p(T) + f_1(t,T)]\frac{dT}{dt} + f(t,T) \tag{1b}$$

$$\Phi(t) = \Phi_{rev} + \Phi_{kin} \tag{1c}$$

where the reversing heat flow is defined by Eq. (2):

$$\Phi_{rev}(t) = \left(\frac{dQ}{dt}\right)^{T}_{rev} = -C_p(T)^{*}\beta \tag{2}$$

i.e. the heat capacity multiplied by the overall rate of temperature change (β). The kinetic heat flow is an unknown function that can be defined according to Eq. (3) using Eq. (1a):

$$\Phi_{kin} = f(T,t) \tag{3}$$

and its slope is

$$a_f = \frac{df(T,t)}{dt} \tag{4}$$

The heat capacity function ($C_p(T)$) is the target of our next investigations. The heat capacity function is produced by the MDSC after deconvolution of the modulated heat flow using Eq. (5):

$$C_p(T)_{T-T(t_3)} = K_{C_p}\frac{\text{smoothed}[A_{HF}(t_3)]}{\text{smoothed}[A_T(t_3)]}\frac{1}{\omega} \tag{5}$$

Schawe [5, 6] discussed the reversing and non-reversing heat flows introduced by Reading and coworkers [1]. Instead of this concept, he defined a complex heat capacity function by analogy with other concepts using periodic or semiperiodic effects in a linear response theory. According to the equations of Schawe [5], at the glass transition temperature Eq. (6) can be developed (Eqs (37) and (39) in his paper):

$$|C|^2 = C'^2 + C''^2 = C'(C_p + C_\infty) - C_p C_\infty \tag{6}$$

Assuming that

$$C_p C_\infty \sim C' C_\infty \tag{7}$$

he obtained:

$$\Phi_{rev}(T,\omega_o) = |C(T,\omega_o)|\beta_o \approx \sqrt{C_p(T)C'(T,\omega_o)}\ \beta_o \tag{8}$$

Schawe also declared in [5], that Eq. (1b) results in a similar conclusion; nevertheless, it has a physically different meaning, i.e. it refers to a kinetically controlled transition of the heat capacities. We can compare Eq. (8) to the expression for the reversing heat flow of the MDSC (Eqs (7) and (8) in [5]):

$$\Phi_{rev}[T(t)] = \frac{\Phi_a[T(t)]}{T_a\omega_o}\beta_o = \sqrt{C_p^2(T) + (a_f/\omega_o)^2}\,\beta_o \tag{9}$$

As a result we get a very similar expression. The numerical values of the solution of Eqs (9) and (8) differ depending on the second term of Eq. (8). If this has a negligible value with respect to the square of the heat capacity, the two expressions result the same numerical value.

Basics of polymer crystallisation

Semicrystalline polymers are generally multiphase systems. The crystalline phase (or phases) are always accompanied by some amorphous phase. During the heating and/or cooling process the heat capacity contains the heat capacities of the individual phases and the changes in the enthalpies when one phase transforms into another one. The heat capacity function of semi-crystalline polymers can be given by the general function expressed by Eq. (10):

$$C_p(T) = \sum_i w_i(T)C_p^i(T) + \sum_{i,j}\frac{dw_i(T)}{dT}\Delta H_{i,j} + ... \tag{10}$$

In the first term of Eq. (10) the heat capacities (C_p^i) of the individual phases (i) are summed using their weight fraction (w_i) within the system. The second term ex-

presses the change in the concentration of the individual phases due to the phase transformations (e.g. melting or crystallisation, or one phase dissolution in another).

The equation expresses the heat capacities in a similar way to Eq. (1b).

Let us investigate now the crystallisation process of the polymers.

On the basis of the folded chain lamellar model of polymeric crystals it is generally accepted that the crystallisation needs supercooling. First some crystalline nuclei will be formed then the nuclei will grow. Turnbull and Fisher [7] (1949) derived the rate of nucleation (I^*) using absolute reaction rate theory (Eq. (11)):

$$I^* = (NkT/h)\exp[-(\Delta G^* + \Delta G\eta)/kT] \tag{11}$$

where ΔG^* is the free enthalpy of crystallisation of a nucleus of critical size and this approaches infinity at the melting temperature according to Eq. (12):

$$\Delta G^* = \frac{42\gamma^2\gamma_e T_m^2}{(\Delta H_f \Delta T \rho_c^2)^2} \tag{12}$$

Here ρ_c is the density of the crystals, γ and γ_c are surface energies of the critical nucleus perpendicular to and parallel with the chains, ΔT is the supercooling, T_m is the melting temperature and ΔH_f is the melting enthalpy of the crystals.

The second term in Eq. (11) expresses the free energy of diffusion across the phase boundary and it can be given by Eq. (13):

$$\Delta G_\eta/kT = a + [b/(T-T_o)] \tag{13}$$

where a and b are empirical constants and T_o is the temperature when no further material transport across the phase boundary take place (near to T_g) [8].

The rate of nucleation decreases to zero with decreasing supercooling. In general it ceases at 10–30 K below the melting temperature. As there is a material transport through a surface during the growth process in this model, Eq. (13) will also work at the growth step, where additional activation energy is necessary to nucleate the next layer on the growing crystalline surface, as well as to add a new segment to the crystallised chain from the molten phase (secondary and tertiary nucleations [8]).

Consequently, the polymer crystallisation in the folded chain crystallisation model can not be a reversible process, it should not give an additional contribution to the $C_p(T)$ function when the polymer melt is cooled. The heat capacities should be the weighted average of those of the different phases.

Summarising the theoretical background we can conclude, that the formation and consequently the melting of the polymeric crystals should appear as a kinetic (non-reversing) rather than a reversing process in the MDSC cell.

In previous studies on polymers by MDSC [4, 9–12] (as well as by oscillating DSC [5]) a reversing heat flow during the melting of crystalline polymers have undoubtedly been detected and measured. Wunderlich [11] showed that the measured heat capacities of semi-crystalline polymers follow the theoretical values calculated on the basis of vibration frequencies up to a critical temperature. Above the critical temperature they deviate positively from the calculated values. He proposed a so-called mesomorphic model for solving the discrepancies. According to his model conformational distortions are formed in the crystalline state and these distortions modify the crystalline state (e.g. transforms the orthorhombic phase of PE into a hexagonal one). This state is called condis crystal and it is defined as a separated phase, i.e. mesophase.

Traditionally mesophase is the term for a phase with an organisation between the organisation of the liquid and the crystalline phases respectively, i.e. it contains some kinds of order with an enhanced mobility of the structural elements. The transitions of a mesophase from one into another or into the liquid state always takes place at a given temperature, like the melting of the crystals and it can be characterised by more or less sharp transition with a finite value of enthalpy. This means that their transitions are first order transitions. The only exception described in the literature is the transition from the Smectic C to the Smectic A phase and vice versa. It is a second order transition [13] with only a step on the DSC curve, similarly to the step in the heat flow curves at the glass transition of polymers. In this case both phases are in a highly fluid state, i.e. they are practically liquids.

The problem with the mesophase model is that a separated mesophase should have distinct thermodynamic properties (melting temperature, melting enthalpy) which are analogous to those of the crystalline materials, although naturally with a much lower numerical value. Therefore the heat capacity will not change continuously with increasing temperature like the heat capacity function in the melting zone of semi-crystalline polymers and this kind of melting process will not show reversible behaviour. There is no second order transition between two phases with different lattice parameters or symmetries. The hexagonal phase of PE has a smaller density than the orthorhombic phase. If locally hexagonal phase would form it would cause a locally extension of the material which is energetically highly unfavourable. Therefore the model proposed by Wunderlich is non acceptable.

Recently Okazaki & Wunderlich [14] studied the reversibility of polymer melting by MDSC and found small amount of reversible melting and crystallisation in poly(ethylene terephthalate) by extending the time used in the quasi-isothermal mode. They found that 'a reversing contribution to the heat capacity is present' although, as they declare it in their paper [14] 'it should not be so'. They planned new experiments to reveal more about the kinetics and mechanism of melting.

Our experiments have been designed to study the reversible part of the melting of semi-crystalline polymers. The reversing heat flow has been measured and analysed as a function of time dependent parameters (heating/cooling rate, modulation period), and annealing experiments have been carried out near to the melting temperature using MDSC. The results of the former experiments are shown in this paper. The annealing experiments will be published elsewhere [15].

We use the word reversing according to the terminology of TA for MDSC and reversible according to the thermodynamics. That is, the heat flow is called reversing, but the transition enthalpy integrated from this heat flow is called reversible.

Experimental

Equipment and experimental conditions

TA Instrument MDSC type 2920 with the Thermal Analyst 2100 computing system was used. The overall heating/cooling rate varied from β=1 to 5 K min^{-1}. At a higher rate of temperature change the transitions are generally expected to be broader.

Different modulation types have been used. As the resolution and optimal noise to signal ratio depends on the local maximal heating/cooling rate, the parameters of the modulation (depth and frequency) were selected to achieve not only 'heating only' or 'cooling only' conditions (tangential modulation, see on Fig. 1) but also a cooling during heating condition (deep modulation on Fig. 1). The heating/cooling capacity of the equipment together with the geometry and heat capacity of the measuring cell determine a maximal depth of modulation possible without destroying the harmonicity of the temperature function. The parameters of the deep modulation were selected according to this restriction. An intermediate heating/cooling type has also been used (medium modulation) in some of the experiments. Here the amplitude of modulation was twice as the amplitude of the 'heating only' modulation.

The frequency of the modulation influences the measured value of the heat capacity, therefore frequency dependent cell constants have been used in the measurements [12]. The heat capacities have been reduced to their zero frequency value and all the Figures given in this paper are based on these reduced values of the experimental heat capacities.

The method used to obtain the transition enthalpies is shown in Fig. 2. The heat capacities as a function of temperature for HDPE, recorded by 'heating only' modulation and with p=15 s, are shown in Fig. 2. The heat capacities on cooling follow a straight line characteristic to the melt until the crystallisation causes a jump in the heat capacities. They approach the heat capacities measured

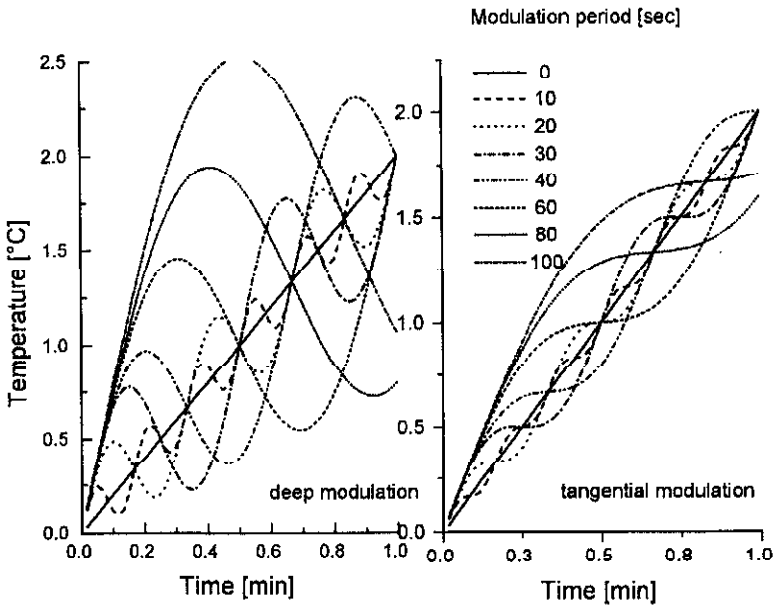

Fig. 1 Temperature *vs.* time of deep and tangential modulation with different modulation period

in the heating cycle and when they return to that value, this temperature is used as the lower limit of the integration in all of the heat flow charts.

Helium was used as the purge gas at a fairly constant 100 ml min^{-1} flow rate. The cell constant have been determined using this flow rate of He [12].

Materials and sample preparation

HDPE HDS148, Kemcor product, an extrusion grade polymer, MFI: 1.0 g $(10\ min)^{-1}$.

LLDPE ET6013, ICI product, an injection moulding grade polymer, MFI: 1.0 g $(10\ min)^{-1}$. Density: 922 kg m^{-3}.

LDPE1 WNCl76, ICI product, a coating grade polyethylene, MFI: 7.6 g $(10\ min)^{-1}$. Density: 919 kg m^{-3}.

LDPE2 XHFl79, ICI product, a blow film grade polyethylene, MFI: 1.0 g $(10\ min)^{-1}$. Density: 921 kg m^{-3}.

VLDPE ETSE9078, Union Carbide product, an injection moulding grade polyethylene, MFI=2.5 g $(10\ min)^{-1}$. Density: 910 kg m^{-3}.

PP GWM22, ICI product, an injection moulding grade polymer, MFI: 4 g $(10\ min)^{-1}$.

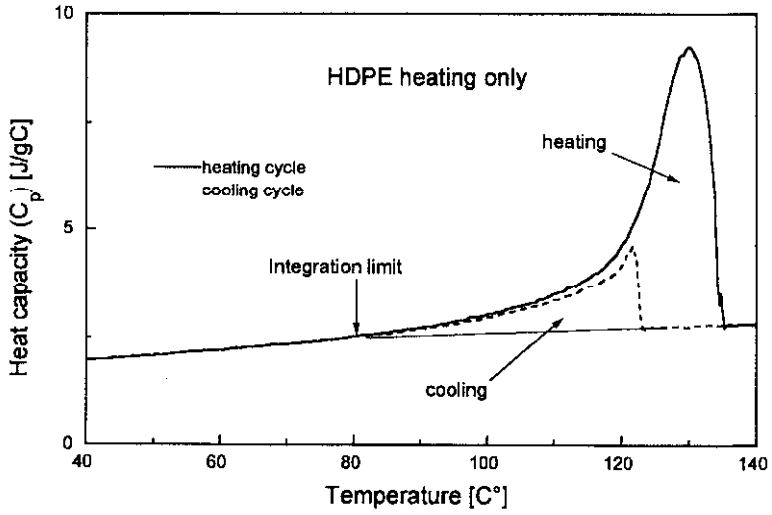

Fig. 2 Heat capacity *vs.* temperature of HDPE for demonstration how to obtain enthalpy values

Samples were cut from injection moulded tensile test bars (prepared with a Johns injection moulding machine), their mass varied from 3–15 mg. A good contact of the sample with the aluminium pan is crucial to assure an undisturbed heat flow (decreasing the kinetic retardation of the heat flow) therefore flat lamellar samples were tested with a circular cross section of 5 mm in diameter. Cylinders were punched out from the test bars then thin sections were cut out from the cylinders using a sharp blade. Skin and core sections of the same sample could be investigated in this way, however, only the core sections were used for this study.

The role of the thermal history in the melting process is well known. All the samples used in this work have been heated above their melting point by 20–30 K and then cooled at a 2 K min^{-1} rate prior to this investigation. This heating/cooling cycle is called a standardising cycle and 'washed out' the thermal history of the samples, hence they had a uniform history (standardised state).

Results and discussion

Exotherm while cooling during the heating cycle

Figure 3 shows the modulated temperature, the modulated heat flow and the calculated DSC curves (total, reversible and kinetic heat flows) of a HDPE using an extreme deep modulation (β=1 K min^{-1}, A_T=1.6 K, p=40 s).

At these conditions of modulation the sample is strongly cooled during heating (Fig. 3). The response of the system to the variable temperature is an alternat-

ing endothermic and exothermic heat flow. The reversible heat flow is present during the whole melting process and it is a remarkable component in the melting peak of the total heat flow.

The Fourier analyses uses a 2 min data package and it is carried out during the recording of the data. Therefore there is a 2 min shift between the primarily recorded data and the calculated data in Fig. 3.

Figure 4 shows the cooling section of the cycle. Here the overall cooling rate (β) was 2 K min^{-1}, A_T=0.6 K and p=60 s. The modulation frequency was inadequate as there was less than three complete modulation cycles during the crystallisation process. This resulted in a peak in the heat capacity during the crystallisation. This peak is an artefact, it can not be analysed as any form of transition heat.

The crystallisation is characterised mainly by kinetic heat flow and this is in good agreement with the expectations. Nevertheless, a reversible process is also present but it is a minor component (~2–3%).

Some important characteristics of the heat flows at the temperature range responsible for the melting (from 70 to 130°C) should be noted:

1. The peak temperature of the reversible heat flow does not correspond to that of the total heat flow.

2. The decrease of the reversing heat flow after its peak is parallel with the sharp increase of the kinetic heat flow.

3. Reversing heat flow starts to increase much before the 'melting peak' could be recognised on the total heat flow.

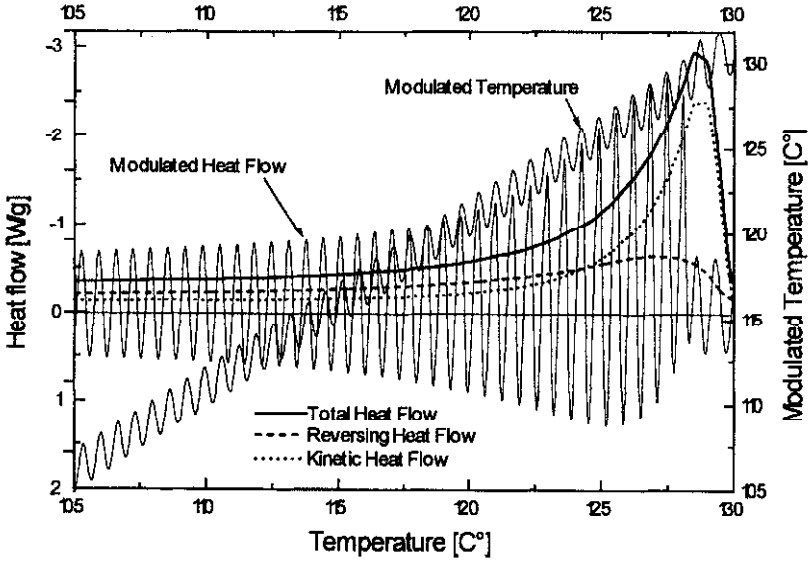

Fig. 3 Primary and calculated data obtained on HDPE using deep modulation. Heating cycle by β=1 K min^{-1}

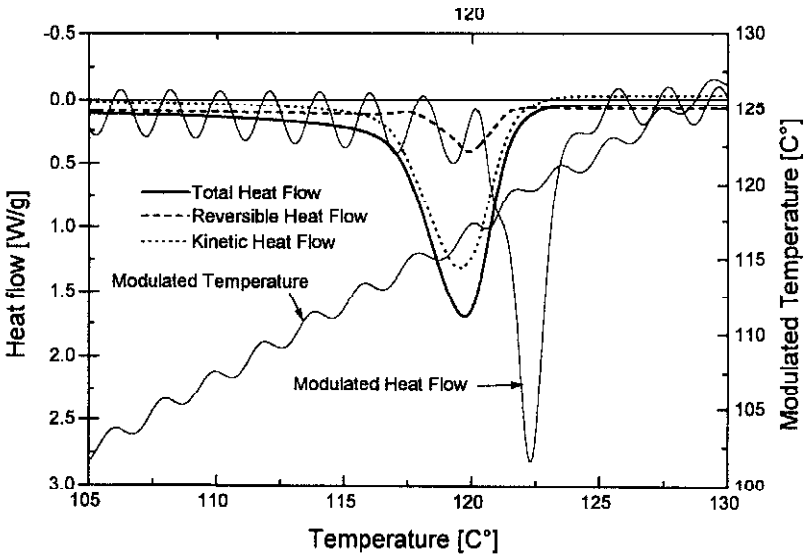

Fig. 4 Primary and calculated data obtained on HDPE using deep modulation. Cooling cycle by β=2 K min^{-1}

Role of the overall heating/cooling rate

Figure 5 shows the total heat flow in HDPE recorded by different heating/cooling rates. Tangential type of modulation and p=40 s modulation period had been selected in this experiment. Four complete cycles have been carried out using (β=2, 5, 5 and 2 K min^{-1} heating and cooling rates. The heat flows are recalculated to the standard β=2 K min^{-1} underlying heating/cooling rate.

There are clearly visible differences between the DSC curves recorded with (and below) β=2 K min^{-1} or above. The cooling parts of the cycles show the characteristics of the cooling rates, the heating parts of the cycles show the effect of the thermal history (cooling rate). The changes in the curve can not be interpreted as decomposition of the material due to the heat treatments above the melting temperatures for a long time, as the curves obtained for the last cooling cycle carried out by β=2 K min^{-1} rate are identical to those obtained for the first cooling cycle.

Figure 6 shows the heat capacities of HDPE recorded in the same cycles. The heat capacity measured on cooling approaches the value of the heating cycle at 60°C. This temperature value was selected as lower limit of integration (Fig. 2). This temperature is the same at all heating rates used in this experiment and it roughly corresponds to the onset of the a relaxation measured e.g. by dynamic mechanical relaxation [16] .

Figure 7 shows the total, the reversible and the kinetic heat flow respectively for the last heating cycle of HDPE shown in Figs 5 and 6. The reversing heat flow

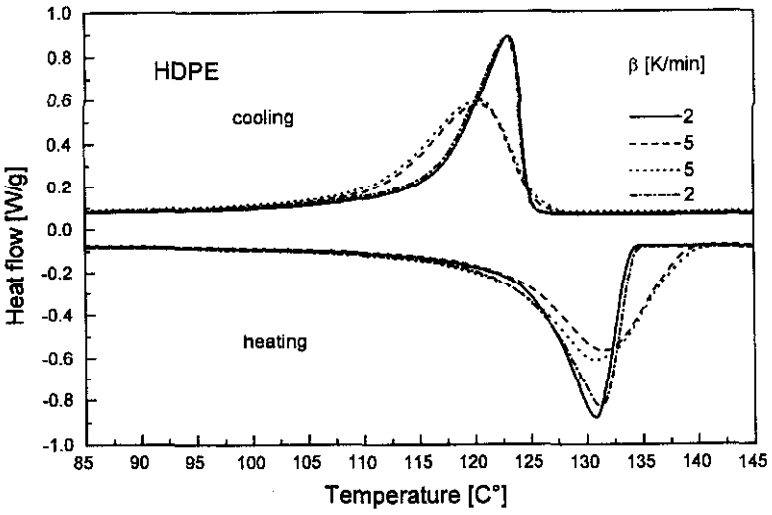

Fig. 5 Total heat flow *vs.* temperature of HDPE using different overall heating and cooling rates

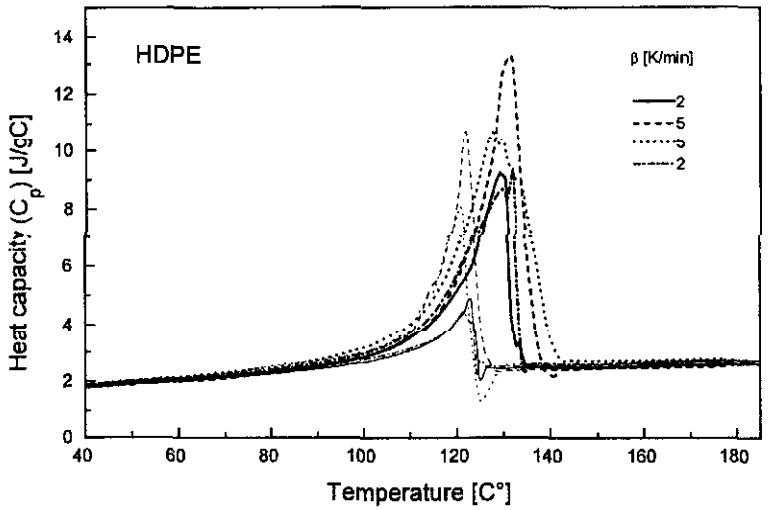

Fig. 6 Heat capacities *vs.* temperature of HDPE using different overall heating and cooling rates

is practically the same as the total heat flow up to 115°C when a kinetic heat flow starts.

Figure 8 shows the derivative of the kinetic heat flow shown in Fig. 7 over the whole temperature range of recordings (i.e. from –120°C). It can be seen that the slope of $f(T,f)$ function (a_f) is generally independent on the temperature and it

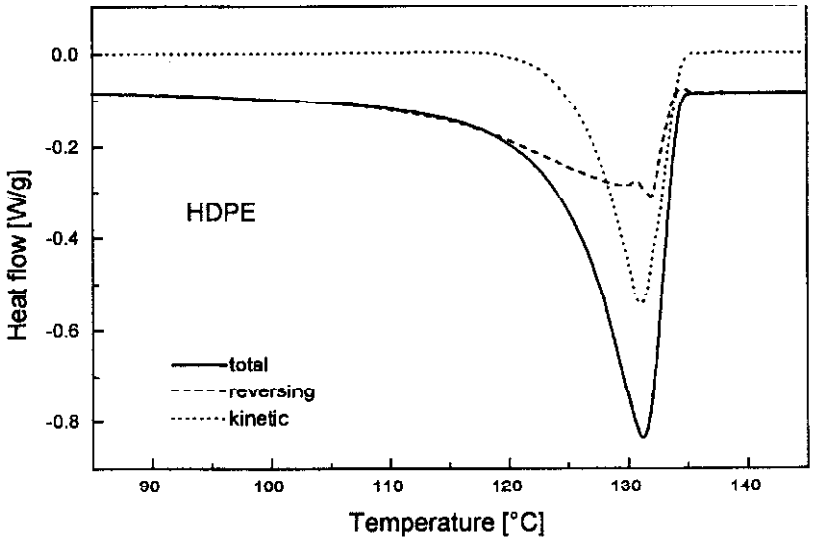

Fig. 7 Total, reversing and kinetic heat flow *vs.* temperature of HDPE

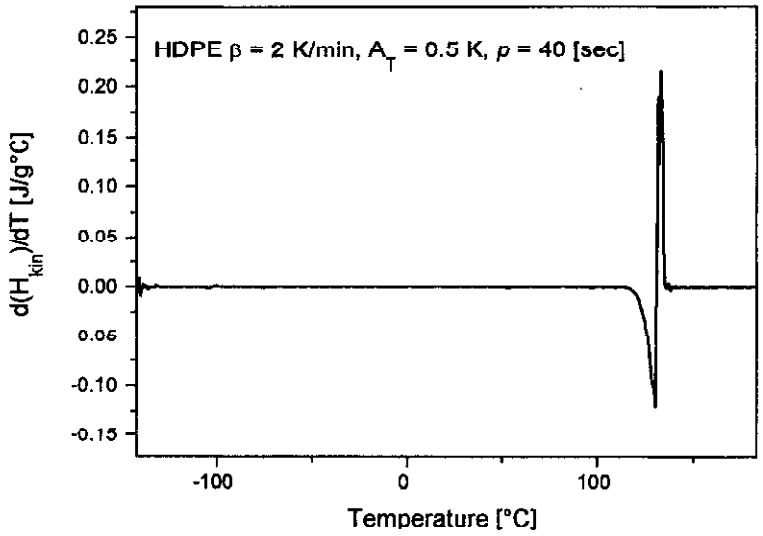

Fig. 8 Derivative of the kinetic heat flow *vs.* temperature of HDPE shown in Fig. 7

is nearly zero for most of the DSC curve. If we compare the two expressions (Eqs 8 and 9) for the reversing heat flow and taking into account that a_f/w_o is very small with respect to C_p ($a_f << 0.01$ [J g^{-1}K^{-1}], $\omega_o \sim 0.06 \div 0.6$ and $C_p > 1$ [J g^{-1}K^{-1}]), the two expressions for the reversible heat flow are numerically identical. The function $f(T,f)$, and its slope change greatly, however, in the melting range of HDPE

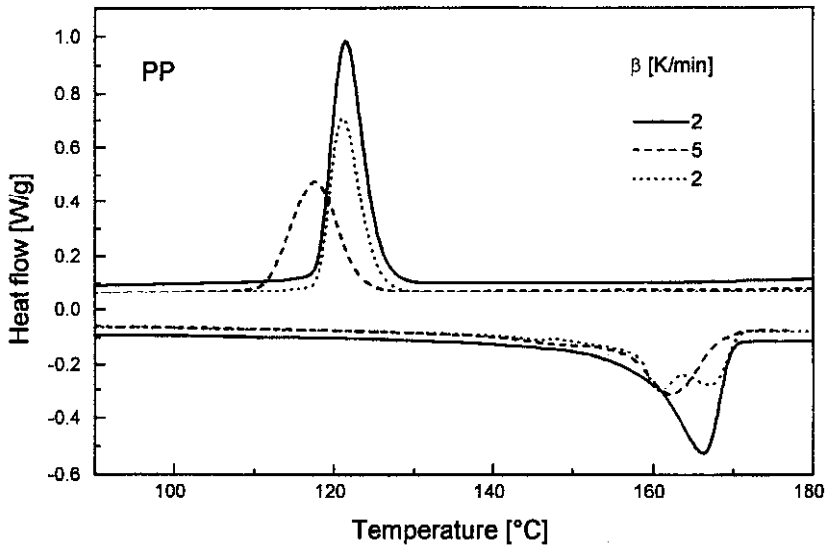

Fig. 9 Total heat flow vs. temperature of PP using different overall heating and cooling rates

(and as we will see later on, this slope change is generally the same for all of the semi-crystalline polymers investigated).

The data approximation by experiments fit equally well both the Reading's and Schawe's. A problem remains with Schawe's assumption [5] the concept of the complex heat capacity function. This does not fit the thermodynamic definition of the heat capacities, as heat capacity is defined as a scalar value.

Similar changes in the total heat flow as a function of the heating rate shown on Fig. 5 for PE, can be seen on the total heat flow charts of PP recorded by different overall heating/cooling rates (Fig. 9).

The role of the frequency of the modulation

DSC curves of the same samples have been recorded using different modulation periods varied from p=10 to 100 s. The amplitudes of modulation have been adjusted to achieve a similar shape of temperature program (Fig. 2). The technical part of this test has been analysed and published elsewhere [12].

Although the total heat flows recorded by different modulation periods are hard to distinguish from each other (Fig. 6 in [12]), there are some deviations at the melting peaks. The measured heat capacities have been recalculated to their extrapolated zero frequency value and reversing heat flows have been calculated from these values. A series of the reversing heat flow charts as function of the modulation period for HDPE using heating only modulation type are shown in Fig. 10.

It is clear from Fig. 10 that the melting range of reversing heat flows depends on the modulation frequency. The onset temperature of the transition has been defined in Fig. 2. The end-temperature of the transition was regarded as the temperature above the melting peak where the heat capacities measured in the cooling part starts to deviate from those of the heating part. The transition enthalpies have been integrated between these temperature values for all of the heat flows.

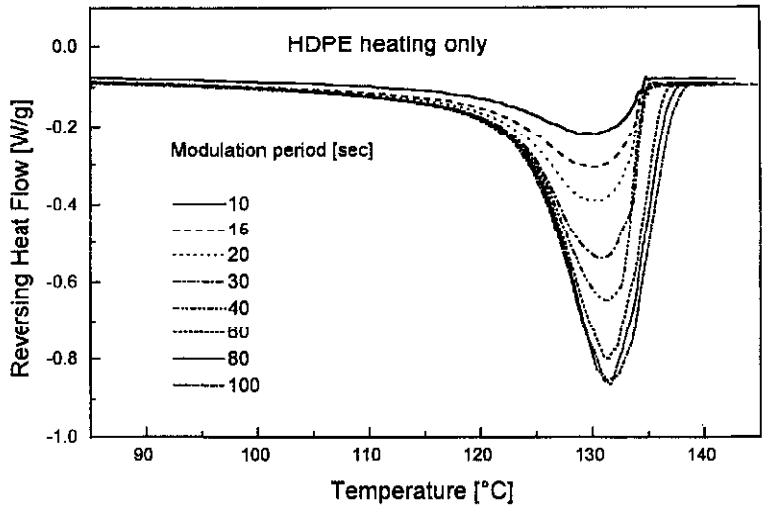

Fig. 10 Reversing heat flow of HDPE measured by different modulation periods

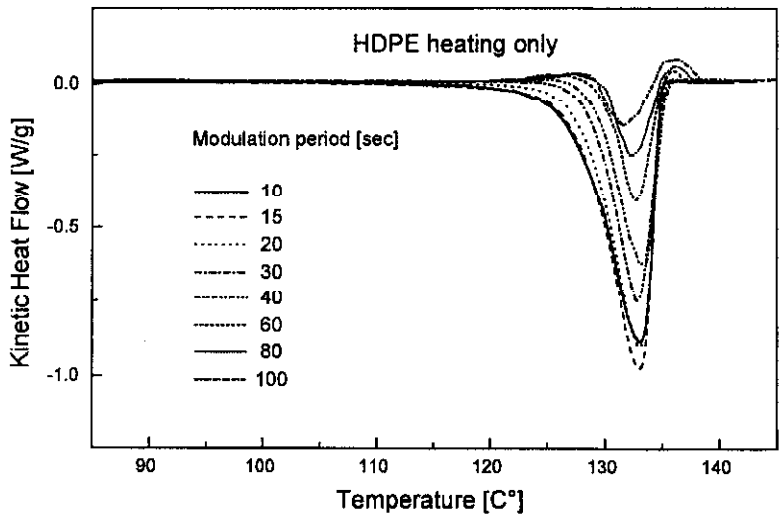

Fig. 11 Kinetic heat flow of HDPE measured by different modulation periods

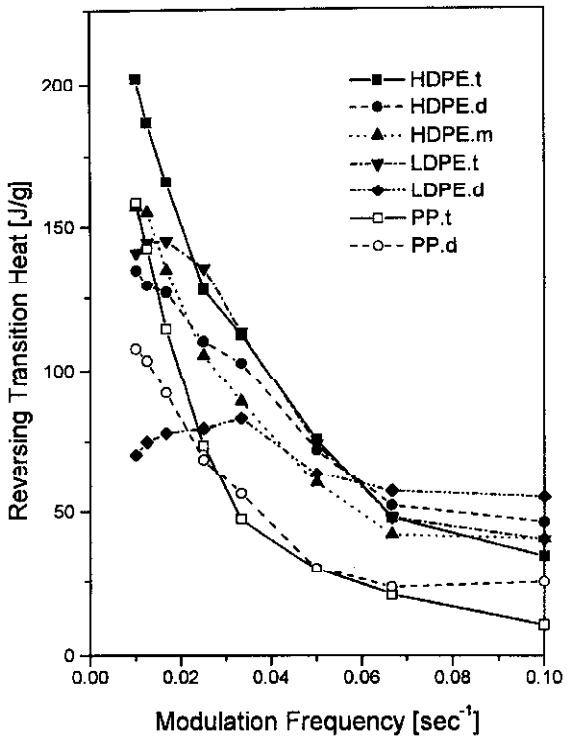

Fig. 12 Enthalpy of melting of different polymers as the sum of reversing and kinetic transitions

Figure 11 shows the corresponding kinetic heat flow charts. The longer the modulation period, the smaller the peak in the kinetic heat flows.

Figures 12–14 show the dependence of the total, the reversing and the kinetic transition enthalpies on the modulation frequency and on the type of the modulation for several polymers.

The reversible enthalpy of melting (as shown on Fig. 12) has been accepted as the difference between the melting enthalpy and the enthalpy of crystallisation. At the starting temperature of the crystallisation when the modulation period was increased there was an additional peak with increasing area for the heat capacities on cooling (Fig. 6), the enthalpy of crystallisation measured using a modulation period of 15 s provided an accurate value which was used to correct data obtained at different modulation periods. The enthalpy of melting obtained from the reversing heat flow curve has a relatively low value at lower periods (p=10–30 s) then it increases with increasing modulation period as seen in Fig. 12. With higher modulation amplitudes, the reversible enthalpy of transition is decreasing. This behaviour clearly shows the relaxation type of the reversible part of the transition.

The enthalpies of melting obtained from the kinetic heat flow charts are shown in Fig. 13. They are complementary to those obtained from the reversing heat flow curves. Figure 14 shows the sum of the reversing and nonreversing melting enthalpies shown in Figs 12 and 13. The enthalpy of melting for the total heat flows do not depend on the modulation period agreeing with the conclusion given in [12].

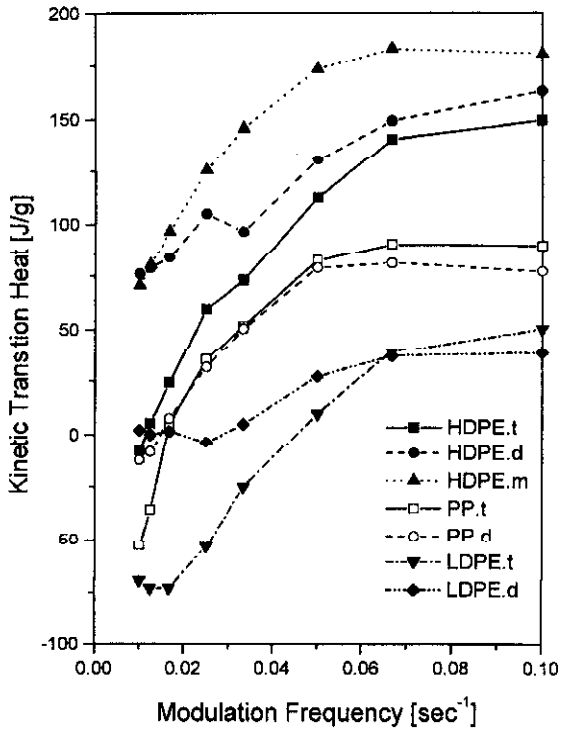

Fig. 13 Enthalpy of melting of different polymers obtained from the reversing heat flow charts

Figure 15 compares the total heat flow curves of different types of polyethylene. The melting temperature and the enthalpy of melting increases with increasing structural regularity in the polymer (LDPE2 is more regular than LDPE1). Figure 16 represents the kinetic heat flows of the same materials. The area under the melting peak increases with increasing regularity of the materials. The lower the density, the lower the ratio of the kinetic transition to the total enthalpy of melting. LDPEs and VLDPE are extremes where the total kinetic transition enthalpy is less than zero. The kinetic component of the melting enthalpy can be arranged in the following order: HDPE>LLDPE>VLDPE>LDPE.

Figure 17 shows the heat capacities of PEs of different types in a complete cycle of heating and cooling. Increasing deviation in the heat capacities from the

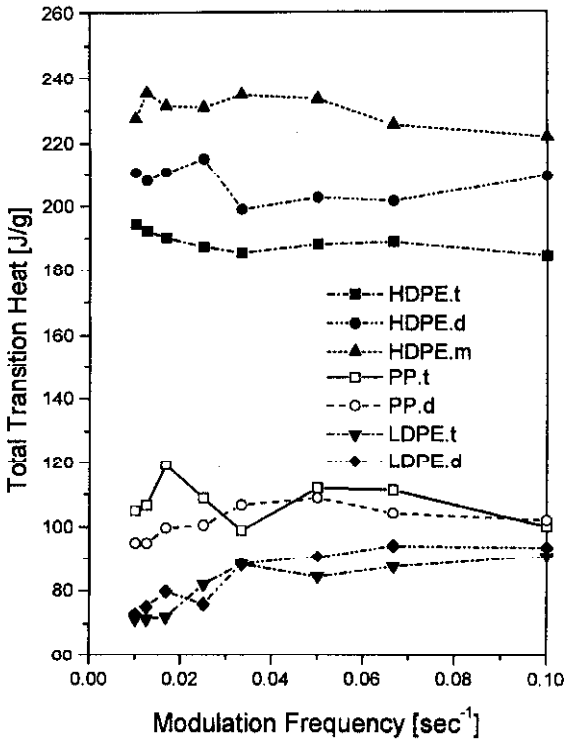

Fig. 14 Enthalpy of melting of different polymers obtained from the kinetic heat flow charts

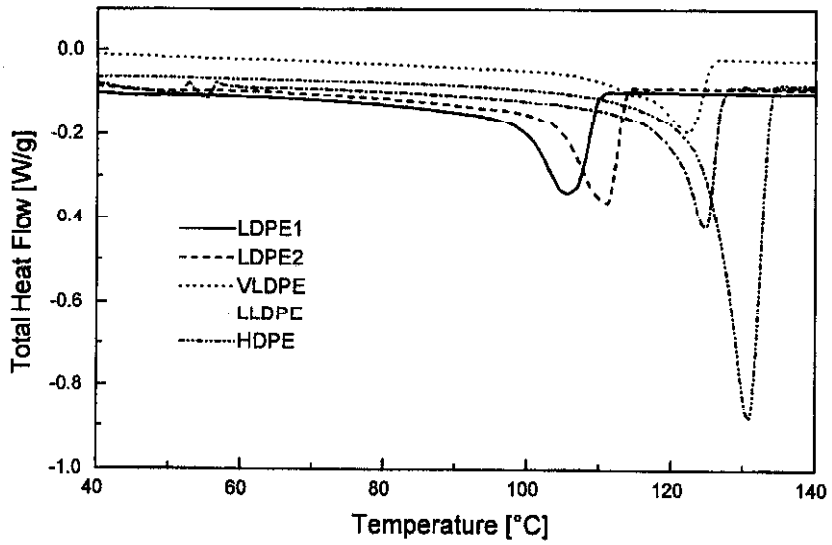

Fig. 15 Total heat flow *vs.* temperature of different types of polyethylene

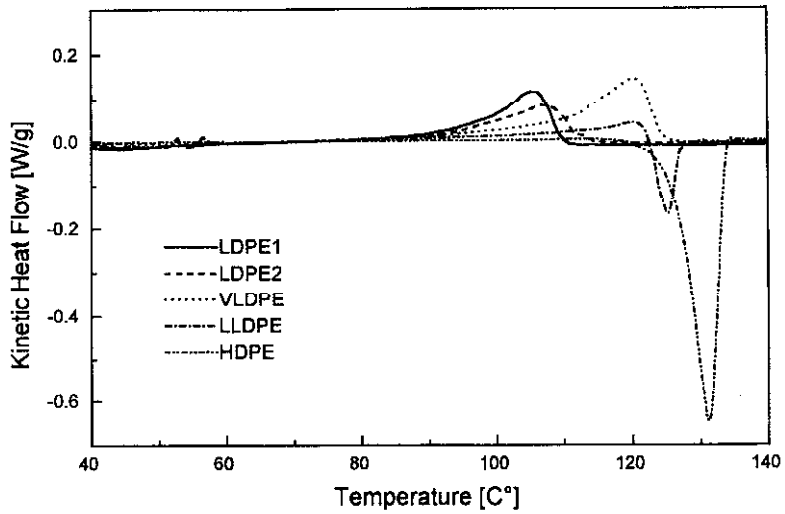

Fig. 16 Kinetic heat flow *vs.* temperature of different types of polyethylene

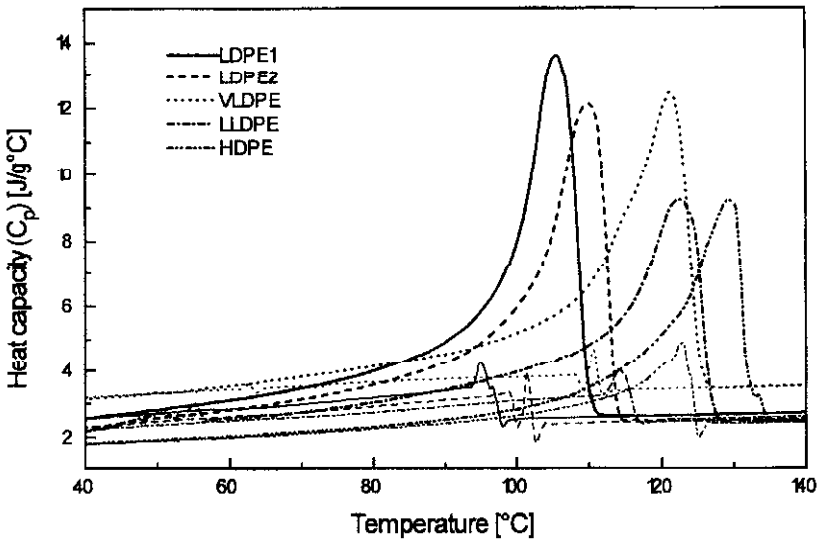

Fig. 17 Heat capacities *vs.* temperature of different types of polyethylene

expected values resulted from increased branching. The lower temperature limit of the integration also decreases with increasing branching. This value is 100°C for HDPE and 40°C for LDPE.

As we have seen above, the crystallisation of the polymers needs supercooling at each types of nucleation, i.e. primary, secondary or tertiary, which means it can not be reversible. Nevertheless, here we observed reversible parts of crys-

tallisation (see step at the heat capacities during the crystallisation on Fig.17). This reversible portion is always present in all of the studied polymers. In polyethylene, the portion of the reversible crystallisation depends on the level of branching. High density (linear) PE has the lowest reversible value, highly branched low density PE has the greatest. Similar can be concluded for the reversible portion of the melting of semi-crystalline polymers. In LDPE, the melting is reversible nearly in 100% of the total transition, and this ratio decreases by increasing density of LLDPE.

Conclusions

The following conclusions can be drawn from this work:

1. The kinetic heat flow and its slope are zero over most of the temperature range with the exception of the melting region. Therefore the reversing heat flow measured by the MDSC and calculated using the Fourier transform of the response of the equipment to the modulated temperature corresponds to the thermodynamically defined heat capacities.

2. There is a time dependent reversing part of the heat flow during the melting process. The longer the time of modulation, the greater is the portion of reversing heat flow within the total heat flow. This dependence shows a relaxation type of transition during the melting process.

3. The reversing part of the melting process depends on the structure of the polyethylene. The greater the branching in the chain, the greater the reversibility. It is a transition part of the heat capacities therefore Eq. (1b) is supported.

4. The mesophase (condis crystal [9]) model does not describe the phenomenon properly. It does not explain the continuous deviation of the measured heat capacities from the expected (calculated) ones. Further studies should be conducted to get a proper explanation of the reversing heat flow during the melting process.

List of symbols

$A_{HF}(t)$ amplitude of instant heat flow signal at t time [mW]
$A_T(t)$ amplitude of the temperature signal at t time [K]
$C(t)$ time dependent heat capacity
C complex heat capacity
C' real part of C
C'' imaginary part of C
C_b time dependent heat capacity measured at scanning rate of b [J $g^{-1}K^{-1}$]
$C_p(T)$ static heat capacity of the sample at constant pressure and T temperature [J $g^{-1}K^{-1}$]
C_∞ heat capacity at high frequencies ($\omega\to\infty$) [J $g^{-1}K^{-1}$]
Q heat [J]

G Gibb's free energy [J mol^{-1}]
h Planck's constant [J cm mol^{-1}]
H enthalpy [J mol^{-1}]
ΔH_f melting enthalpy of crystal [J mol^{-1}]
i imaginary unit
I^* rate of nucleation [s^{-1}]
k gas constant [J K mol^{-1}]
N Avogadro's number [6.02·10^{23} mol^{-1}]
t time [s]
t_3 time at three half periods [s]
T temperature [K]
T_m melting temperature [K]
T_c temperature of crystallisation [K]
T_g glass transition temperature [K]
ΔT supercooling, T_m–T_c [K]
p period of sinusoidal signal [s]
β temperature change [K min^{-1}]
β_o scanning rate [K min^{-1}]
γ surface energy at the side of the crystalline nuclei [J m^{-2}]
γ_e surface energy at the end of the crystalline nuclei [J m^{-2}]
Φ heat flow [mW]
Φ_a amplitude of oscillating heat flow [mW]
Φ_{rev} reversing component of Φ [mW]
ρ_c density of the crystal [kg m^{-3}]
ω angular frequency [s^{-1}]
ω_o angular frequency of the measurement [s^{-1}]
$f(T,t)$ time dependent function which describes the kinetic component of the measured signal [mW]

* * *

The authors are indebted to prof. R. A. Shanks (Dept. Applied Chemistry, RMIT, Melbourne) for their comments and for the discussion on the topics.

References

1 M. Reading, D. Elliott and V. L. Hill, J. Thermal Anal., 40 (1993) 949.
2 P. S. Gill, S. R. Sauerbrunn and M. Reading, J. Thermal Anal., 40 (1993) 931.
3 A. Boller, Y. Jin and B. Wunderlich, J. Thermal Anal., 42 (1994) 307.
4 B. Wunderlich et al., Modulated Differential Scanning Calorimetry: Summary of Eqs and Derivations Needed for the Understanding of MDSC, for internal use of the ATHAS Group, November 8, 1995.
5 J. E. K. Schawe, Thermochim. Acta, 260 (1995) 1.
6 J. E. K. Schawe, J. Thermal Anal., submitted for publication (1996) (referred in [4]).
7 D. Turnbull and J. C. Fisher, J. Chem. Phys., 17 (1949) 71.
8 B. Wunderlich, Macromolecular physics, Vol. II. Academic Press, New York 1976.
9 F. Cser, Reversible Melting and Crystallisation of semi-crystalline Polymers. Poster paper presented at 10th National Convention of RACI. Adelaide, 27 September–2 October, 1995, P99, Program Booklet p.149.

10 F. Cser, F. Rasoul and E. Kosior, Reversible Melting and Crystallisation of semi-crystalline Polymers. Paper presented at 22nd Australasian Polymer Symposium, Auckland, 3–5 February, 1997. Preprints p.
11 B. Wunderlich, Macromol. Symp., 98 (1995) 1069.
12 F. Cser, F. Rasoul and E. Kosior, J. Thermal Anal., 50 (1997) 727.
13 P. G. De Gennes, The Physics of Liquid crystals, Univ. Press, Oxford 1974.
14 I. Okazaki and B. Wunderlich, Macromolecules, 30 (1997) 1758.
15 F. Cser, F. Rasoul and E. Kosior, J. Thermal. Anal., (to be published).
16 N. G. McCrum, B. E. Read and G. Williams, Inelastic and Dielectric Effects in Polymeric Solids, Wiley, New York 1983.